Langmuir−Blodgett Films of a Novel Cellulose Derivative with Dihydrophytyl Group: The Ability to Anchor β-Carotene Molecules

Keita Sakakibara,*,† Shinsuke Ifuku,† Yoshinobu Tsujii,‡ Hiroshi Kamitakahara,† Toshiyuki Takano,† and Fumiaki Nakatsubo†

Division of Forest and Biomaterials Science, Kyoto University, Kitashirakawa Oiwake-cho, Sakyo-ku, Kyoto 606-8502, Japan, and Institute for Chemical Research, Kyoto University, Uji, Kyoto 611-0011, Japan

Received January 27, 2006; Revised Manuscript Received March 30, 2006

A novel cellulose derivative, 6-*O*-dihydrophytylcellulose (DHPC), was first synthesized via a ring-opening polymerization and allowed to self-assemble onto an air−water interface. Langmuir−Blodgett (LB) films were characterized with atomic force microscope (AFM), UV−vis spectroscopy, and Fourier transform infrared spectroscopy. The surface pressure−area (π−A) isotherms for DHPC and β-carotene (β-C) mixture indicated strong interaction between these compounds to pack well. Thus, DHPC has the ability to anchor β-C in the monolayer. It was proved that a β-C−DHPC monolayer was transferred successfully onto a substrate, yielding Y-type LB films by UV spectroscopic analysis. The transmission and reflection−absorption IR spectra (RAS) indicated that the dihydrophytyl chains had almost trans-zigzag conformation and were oriented nearly perpendicular to the substrate. AFM section analysis revealed the thickness per layer to be 2.32 nm. Consequently, DHPC was found to be an appropriate matrix to fabricate the mixed LB films containing β-C.

Introduction

Cellulose derivatives have broad potential to design more advanced polymeric materials such as liquid crystalline polymers,[1] well-defined multilayered assemblies,[2] selective membranes,[3] sensor matrixes,[4] recognition devices,[5] luminescent polymers,[6] organic−inorganic complex materials,[7] bioactive and biocompatible materials,[8] and optoelectronic devices[9,10] because of their specific structure: strictly linear (1→4)-β-glucan structure and three reactive hydroxyl groups per anhydro glucose unit (AGU). One of the interesting attempts is the introduction of hydrophobic side chains onto cellulose yielding an amphiphilic polymer that may possibly form a stable monolayer.[11] The monolayers of cellulose derivatives are expected to be thermally and mechanically stable owing to the semiflexiblility of the cellulose main chain.[12,13] Langmuir−Blodgett films composed of cellulose derivatives, therefore, would be an attractive biomaterial: These can be used to build up well-defined supramolecular architectures. Although cellulose derivatives could be used as starting materials suitable for preparing LB films, they are useful in the construction of complex architectures: the incorporation of guest molecules or of covalently attached functional groups without destroying the regularity and homogeneity of multilayers.[14,15]

For several decades, LB films containing major chloroplast pigments have been proposed to serve as models of photosynthesis. In particular, LB films of chlorophyll a have received considerable interest as a model to investigate chloroplast thylakoid, the structural unit of photosynthesis.[16−21] The central issue in photosynthesis is the process of light-induced charge separation whereby light energy is converted into chemical energy. Chlorophyll a is a principal pigment in this energy transduction.[22] Its characteristic features, from the viewpoint of their molecular organization processes, are the central metal of the tetrapyrrole macrocycle[23] and the phytyl chain.[24,25] This long hydrocarbon side chain is assumed to be relevant not only for hydrophobicity of the molecule but also for specific interactions with carotenoids noncovalently[26] and a high affinity for hydrophobic environments.[24,25] It is well-known that chlorophyll molecules on grana thylakoid membranes are arranged in a highly ordered state and that the local concentration of porphyrin ring is relatively high. Hence, the phytyl group is expected to make these pigments self-assemble into a supramolecular system on the membrane.

Until now, there have been few studies of LB films containing natural pigments which are anchored and stabilized by a matrix of a strong polymer. Sato et al. reported the morphological and molecular structure of LB films of chlorophyll a in detail, though the photoelectrochemical behavior of the films was not investigated.[19,20] To the contrary, Miyasaka et al. reported the photoelectrochemical behavior of chlorophyll mixed monolayers,[27,28] though the matrix used was stearic acid or lecithin. Matsuura et al. reported the fabrication of LB films of β-carotene, though a β-carotene monolayer was transferred onto only hydrophilic substrates and the fabrication technique was rather difficult.[29]

Our final goal is to fabricate a novel biomimetic photochemical energy conversion system using a supramolecular structure of cellulose derivatives. In the initiation step, we planned to examine the stacking of natural pigments with an isoprenoid moiety, such as chlorophyll a and β-carotene, in the matrix of cellulose derivatives.

In this study, we first prepared a novel cellulose derivative with a dihydrophytyl group, 6-*O*-dihydrophytylcellulose (DHPC), via a ring-opening polymerization, since the dihydrophytyl group is expected to anchor natural pigments with an isoprenoid

* To whom correspondence should be addressed. Phone: +81-75-753-6256. Fax: +81-75-753-6300. E-mail: k_sakaki@kais.kyoto-u.ac.jp.
† Division of Forest and Biomaterials Science.
‡ Institute for Chemical Research.

10.1021/bm060083x CCC: $33.50
Published on Web 05/19/2006

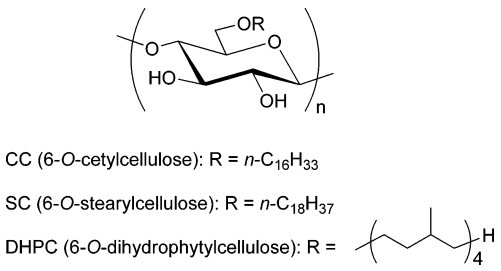

Figure 1. Chemical structures of 6-*O*-substituted cellulose derivatives.

moiety: The reason we select the dihydrophytyl group is that the commercially available phytol is the mixture of E/Z isomers. Second, the surface pressure−area ($\pi-A$) isotherm behavior of DHPC was studied in comparison with those of 6-*O*-cetylcellulose (CC) and 6-*O*-stearylcellulose (SC); CC has the same length of the main chain as DHPC; SC was proven to be a suitable material for preparing LB films, though the stacking ability was not discussed in the previous report (Figure 1).[30] Third, the ability of DHPC to anchor β-carotene (βC) was studied. Finally, we fabricated and analyzed the LB films of βC−DHPC. This paper is the first report to describe the availability of DHPC as a matrix of βC and the fabrication of the mixed LB films. The βC molecules in this fabrication may function as a molecular wire,[31] since βC is a conjugated molecule which provides electric conduction to an organic monolayer.[32]

Experimental Section

Materials. Phytol (97%) was purchased from Aldrich and was used without further purification. Dihydrophytyl tosylate[33] was synthesized by the reaction of dihydophytol[34] with tosyl chloride in the presence of (dimethylamino)pyridine (DMAP) in dichloromethane at room temperature. The other reagents were purchased from Nakarai Tesque, Inc. (Kyoto, Japan) or Wako Pure Chemical Industries, Ltd. (Osaka, Japan). The products were purified with silica gel column chromatography (Wakogel C-200, Wako Pure Chemical Industries). The gel for size exclusion chromatography (Sephadex LH-20) was purchased from Pharmacia. The standard workup procedure included diluting with ethyl acetate or chloroform, washing with distilled water and brine, drying over Na_2SO_4, and concentrating in vacuo.

Measurements. ^{1}H and ^{13}C NMR spectra were recorded with a Varian Inova 300 FT-NMR (300 MHz) spectrometer in chloroform-*d* with tetramethylsilane (Me_4Si) as an internal standard. Chemical shifts (δ) and coupling constants (J) are given in parts per million and hertz, respectively. Optical rotations were measured at 25 °C using a JASCO Dip-1000 digital polarimeter. Number-average molecular weight of the polymer was analyzed by gel permeation chromatography (GPC) in chloroform at 40 °C. Calibration curves were obtained with polystyrene standards (Shodex). A Shimadzu liquid chromatography injector (LC-10ATvp), a Shimadzu column oven (CTO-10Avp), a Shimadzu ultraviolet−visible detector (RID-10A), a Shimadzu refractive-index detector (RID-10A), a Shimadzu communication bus module (CBM-10A), a Shimadzu LC workstation (CLASS-LC10), and Shodex columns (KF802, KF802.5 and KF805) were used. The flow rate was 1.0 mL min^{-1}.

AFM images of a monolayer film deposited on a freshly cleaved mica substrate (15 × 7 mm^2) at pressures of 0, 10, and 30 mN m^{-1} at 20 °C were performed using an NV 2000 (Olympus). Measurements were carried out in tapping mode using a tetrahedral-shaped silicon cantilever (AC240TS−C1, Olympus) with a spring constant of 2 N m^{-1}.

The UV−vis spectra were measured by a Jasco V-560 spectrophotometer, using 75 × 25 × 1 mm^3 quartz plates as a substrate. The infrared spectra were recorded on a Shimadzu 8600 PCs FT-IR spectrometer with a resolution of 4 cm^{-1}. The substrate for transmission spectroscopy was a 38 × 13 × 1 mm^3 CaF_2 plate. For RAS measurement, a Shimadzu RAS-8000 reflection attachment was used at an angle of incidence of 70°, together with a Shimadzu GPR-8000 wire-grid polarizer. For the RAS, glass slides (76 × 26 × 1 nm^3) coated with ca. 75-nm-thick Au films by vapor deposition were used as substrate.

The film thickness was determined according to the procedure described in Ejaz et al.[35] The film was scratched, and the height difference between the scratched and unscratched regions was measured by AFM. A silicon wafer was used as a substrate, which was made hydrophobic in a manner similar to Tsujii et al.[36] It was confirmed that the substrate had no damage by the scratching procedure.

Preparation of a Monolayer Film and Surface Pressure Measurements. A diluted solution of the cellulose derivatives (1 × 10^{-3} M per AGU) in chloroform/methanol (20:1, v/v) was spread onto a water subphase in a Teflon-coated trough (100 × 250 × 5 mm^3, FSD-300, USI-system). The ultrapure water at a normal resistance Milli-Q purification of 18.2 Ω cm (Simpli Lab, Millipore) was used for the subphase. The subphase temperature was kept constant by circulating thermostated water. The surface pressure was measured using a film balance of a Wilhelmy type. After prescribed times were allowed for the solvent to evaporate off, the $\pi-A$ isotherms were measured at a constant compression rate of 6 mm min^{-1}. The vertical dipping method was used to deposit the surface monolayer onto a substrate. The upward and downward stroke rate was 10 mm min^{-1} together. During the deposition, the surface pressure was controlled to remain at 30 mN m^{-1}, and the surface temperature was kept at 20 °C to prepare the LB films. All substrates were cleaned in a 5% aqueous detergent (Scat-20X-N, Nakarai Tesque, Inc.) for 24 h and then placed in acetone, chloroform, acetone, and then water in an ultrasonic bath for 15 min each.

Preparation of DHPC. *3-O-Benzyl-*α*-D-glucopyranose 1,2,4-Orthopivalate (2).* To a solution of compound **1**[37] (670 mg, 1.59 mmol) in dioxane−methanol (4:1, v/v) (7.0 mL) was added 28% sodium methoxide in methanol (0.27 mL, 4.78 mmol). The solution was stirred at room temperature overnight. The reaction mixture was worked up by the standard procedure to give a colorless solid (536 mg, 99%). $[\alpha]_D^{25}$ +34.61° (*c* 1.0, chloroform). ^{1}H NMR ($CDCl_3$, δ): 1.03 (9H, s, $-C(CH_3)_3$), 3.82 (1H, dd, J_{gem} = 11.4, $J_{5,6a}$ = 5.6, C_6-H_a), 3.95−4.02 (1H, C_6-H_b), 3.97 (1H, broad d, $J_{3,4}$ = 4.6, C_4-H), 4.22 (1H, dd, $J_{2,3}$ = 2.1, $J_{3,4}$ = 4.6, C_3-H), 4.41 (1H, m, C_2-H), 4.50 (1H, broad t, $J_{5,6}$ = 5,6, C_5-H), 5.80 (1H, d, $J_{1,2}$ = 5.1, C_1-H), 4.67 (2H, s, $-CH_2C_6H_5$), 7.26−7.39 (5H, m, aromatic). ^{13}C NMR ($CDCl_3$, δ): 97.6 (C-1), 71.8, 72.1, 71.3, 77.4, 62.9, 72.4 (C-2, C-3, C-4, C-5, C-6, -$CH_2C_6H_5$), 123.3 (orthopivalate quaternary carbon), 24.8 [orthopivalate-C(CH_3)$_3$], 35.7 [orthopivalate-$C(CH_3)_3$], 127.7, 128.3, 128.7, 136.9 (aromatic).

*3-O-Benzyl-6-O-dihydrophytyl-*α*-D-glucopyranose 1,2,4-Orthopivalate (3).* To a solution of compound **2** (360 mg, 1.07 mmol) in THF−DMF (4:1, v/v) was added dihydrophytyl tosylate[33] (484 mg, 1.07 mmol) and sodium hydride (128 mg, 3.21 mmol) at 0 °C in light shielding. After 24 h, the reaction mixture was worked up to afford yellow oil. The oil was purified on a silica gel column eluted with ethyl acetate/ *n*-hexane (1:19, v/v) to give colorless oil (571 mg, 87%). $[\alpha]_D^{25}$ +16.03° (*c* 1.0, chloroform). ^{1}H NMR ($CDCl_3$, δ): 0.78−0.92 (15H, 3× s, dihydrophytyl−CH_3), 1.03 (9H, s, piv-H), 0.97−1.60 (24H, m, dihydrophytyl-H), 3.49−3.58 (2H, m, $-OCH_2-$), 3.52−3.80 (2H, m, C_6-H), 3.95 (1H, broad d, $J_{3,4}$ = 4.8, C_4-H), 4.28 (1H, dd, $J_{2,3}$ = 2.4, $J_{3,4}$ = 4.8, C_3-H), 4.41 (1H, m, $J_{1,2}$ = 4.8, $J_{2,3}$ = 2.4, $J_{2,4}$ = 2.4, C_2-H), 4.55 ($J_{5,6}$ = 6.9, broad t, C_5-H), 5.77 (1H, d, $J_{1,2}$ = 4.8, C_1-H), 4.64 (2H, s, $-CH_2C_6H_5$), 7.26−7.39 (5H, m, aromatic). ^{13}C NMR ($CDCl_3$, δ): 97.6 (C-1), 72.1, 71.2, 71.6, 75.7, 69.9, 71.9 (C-2, C-3, C-4, C-5, C-6, -$CH_2C_6H_5$), 123.0 (orthopivalate quaternary carbon), 24.9 [orthopivalate−C(CH_3)$_3$], 35.7 [orthopivalate−$C(CH_3)_3$], 127.4, 128.0, 128.5, 137.5 (aromatic), 19.6, 19.7 (dihydrophytyl −CH_3), 22.6,

Scheme 1. Synthetic Route for DHPC[a]

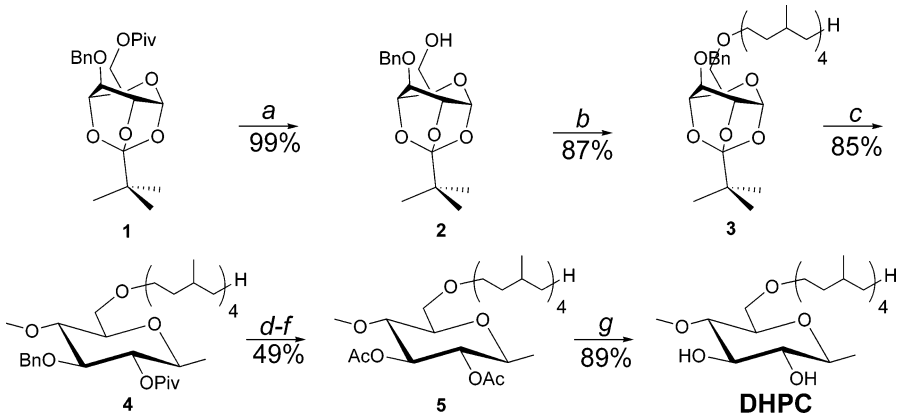

[a] (a) NaOMe, dioxane−MeOH (4:1, v/v) RT, overnight. (b) dihydrophytyl tosylate, NaH, *n*-Bu_4NI, THF−DMF (4:1, v/v), 0 °C, overnight. (c) BF_3-Et_2O, toluene, 0 °C, 48 h. (d, g) NaOMe, THF−MeOH (4:1, v/v), RT, overnight. (e) H_2, $Pd(OH)_2$ on carbon, THF−AcOH (1:1, v/v), 4.4 MPa, RT, 3 h. (f) Ac_2O−pyridine (1:1, v/v) 50 °C, overnight.

22.7, 24.3, 24.5, 28.0, 29.8, 32.5, 36.6, 36.7, 37.3, 37.4, 39.3 (dihydrophytyl $-CH_2-$, $-CH-$) 71.2 (dihydrophytyl-OCH_2-).

*3-O-Benzyl-6-O-dihydrophytyl-2-O-pivaloyl-(1→ 4)-β-D-glucopyranan (**4**).* All these polymerizations were carried out under a high-vacuum line capable of maintaining a vacuum of 1×10^{-3} Torr.[29,38,39] Monomer **3** was dried in a polymerization ampule by evacuating approximately for a day. Dichloromethane and toluene were dried over CaH_2, distilled, and degassed by freezing and thawing three times in a high-vacuum line. All solvents were transferred under high vacuum. The reaction apparatus was then separated by melting off and placed in a bath of the appropriate temperature. BF_3-Et_2O was added into the reaction ampule by a syringe. Polymerizations were terminated by adding cold methanol at the polymerization temperature. After dilution with ethyl acetate, the reaction mixture was worked up to give a colorless solid. This was dissolved in chloroform and then poured into 15-fold amounts of *n*-hexane to precipitate a polymer. The precipitated polymer was filtered and collected to give 3-*O*-benzyl-6-*O*-dihydrophytyl-2-*O*-pivaloyl-(1→4)-β-D-glucopyranan (**4**), mp 112−120 °C, $[\alpha]_D^{25}$ −4.24 ° (*c* 1.0, chloroform). ^1H NMR ($CDCl_3$, δ): 0.81−0.91 (15H, 3× s, dihydrophytyl$-CH_3$), 0.98 (9H, s, piv-H), 0.97−1.60 (24H, m, dihydrophytyl-H), 3.03−3.30 (3H, m, $-OCH_2-$, C_5-H), 3.40−3.53 (3H, m, C_3-H, C_6-H), 3.97 (1H, s, C_4-H), 4.40−4.56 (2H, m, C_1-H, $-CH_2C_6H_5$), 4.95 (1H, s, C_2-H), 5.14 (1H, s, $-CH_2C_6H_5$), 7.11−7.35 (5H, m, aromatic). ^{13}C NMR ($CDCl_3$, δ): 100.0 (C-1), 72.7, 82.0, 75.7, 74.5, 68.6, 74.2 (C-2, C-3, C-4, C-5, C-6, -$CH_2C_6H_5$), 126.9, 128.1, 139.6 (aromatic), 27.7 [orthopivalate−C(CH_3)$_3$], 37.8 [orthopivalate−C(CH_3)$_3$], 176.8 (C═O), 19.9, 20.0 (dihydrophytyl $-CH_3$), 22.9, 23.0, 24.6, 24.8, 25.1, 28.2, 30.2, 33.1, 37.0, 38.8, 39.6 (dihydrophytyl $-CH_2-$, $-CH-$) 70.4 (dihydrophytyl $-OCH_2-$).

*2,3-Di-O-acetyl-6-O-dihydrophytyl-(1→4)-β-D-glucopyranan (**5**).* To a solution of compound **4** (250 mg) in THF−methanol (4:1, v/v) (25 mL) was added 28% sodium methoxide in methanol (0.16 mL). The reaction mixture was kept at reflux temperature for 5 h, treated with Dowex 50-W (H^+) (cation exchange resin, Dow Chemical Co.) for neutralization, and filtered off. The resin was washed with methanol/chloroform (1:4, v/v). The combined washings and filtrate were concentrated to dryness. The product was treated with acetic anhydride and pyridine at 50 °C overnight and concentrated to dryness. To a solution of the polymer in THF/acetic acid (4:1, v/v) (4.5 mL) was added palladium hydroxide on carbon (300 mg). The reaction mixture was stirred under 4.4 MPa of H_2 gas at 50 °C for 5 h. The mixture was concentrated, treated with acetic anhydride and pyridine at 50 °C overnight, and concentrated to dryness. The product was dissolved in chloroform and then poured into 15-fold amounts of ethanol to precipitate a polymer.

Finally, the acetylated polymer was purified by gel permeation chromatography (LH-20) eluted with methanol/chloroform (1/4, v/v) to give 2,3-di-*O*-acetyl-6-*O*-dihydrophytyl-(1→4)-β-D-glucopyranan (**5**) (105.5 mg, 49% overall yield from compound **4**), mp 148−155 °C (dec), $[\alpha]_D^{25}$ −10.4° (*c* 1.0, chloroform). ^1H NMR ($CDCl_3$, δ): 0.83−0.88 (15H, 3× s, dihydrophytyl−Me−H), 1.02−1.60 (24H, m, dihydrophytyl−H), 1.99 (6H, s, C═O−CH_3), 3.19 (1H, s, C_5-H), 3.42 (2H, s, $-OCH_2-$), 3.62 (1H, s, C_6-H), 3.92 (1H, s, C_4-H), 4.42 (1H, s, C_1-H), 4.80 (1H, s, C_2-H), 5.02 (1H, s, C_3-H). ^{13}C NMR ($CDCl_3$, δ): 99.7 (C-1), 71.3, 72.9, 74.5, 73.4, 67.9 (C-2, C-3, C-4, C-5, C-6), 170.1, 176.3 (C═O), 19.6 (dihydrophytyl$-CH_3$), 22.7, 24.5, 24.9, 27.2, 27.9, 30.0, 30.2, 32.8, 37.3, 38.7, 39.3 (dihydrophytyl$-CH_2-$, $-CH-$), 70.0 (dihydrophytyl$-OCH_2-$).

6-O-dihydrophytyl-(1→4)-β-D-glucopyranan (DHPC). To a solution of compound **5** (51 mg) in THF−methanol (4:1, v/v) (10 mL) was added 28% sodium methoxide in methanol (0.075 mL). The reaction mixture was kept at room temperature for 24 h, then at 50 °C for 2 h, neutralized with acetic acid, and concentrated to dryness. The colorless solid product was dissolved in chloroform and then poured into a large amount of ethanol to precipitate a polymer. The precipitated polymer was collected by filtration to give DHPC (38.7 mg, 89%), mp 195−202 °C (dec), $[\alpha]_D^{25}$ −3.45° (*c* 0.50, chloroform). ^{13}C NMR [$CDCl_3$−CD_3OD (20:1, v/v), δ]: 103.0 (C-1), 72.6, 74.6, 80.1, 73.6, 68.8 (C-2, C-3, C-4, C-5, C-6), 19.2 (dihydrophytyl$-CH_3$), 22.2, 24.1, 24.4, 27.6, 29.6, 32.4, 36.2, 37.1, 39.0 (dihydrophytyl$-CH_2-$, $-CH-$), 70.0 (dihydrophytyl$-OCH_2-$).

Results and Discussion

Preparation of DHPC. The preparation of 6-*O*-dihydrophytylcellulose (DHPC) by the modified method of Nakai et al.[40] is shown in Scheme 1. 3-*O*-Benzyl-α-D-glucopyranose 1,2,4-orthopivalate (**2**) was prepared by the depivaloylation of the ortho ester derivative **1** in a 99% yield.[37] The dihydrophytylation of compound **2** was carried out with NaH and dihydrophytyl tosylate in THF−DMF (4:1, v/v) to afford compound **3** in a 88% yield. The polymerization results are summarized in Table 1. All these polymerizations were carried out in a high-vacuum system as previously reported[38] and in the presence of 5 mol % BF_3-Et_2O as an acid catalyst for 48 h. The number-average molecular weights (M_n) of the products polymerized in toluene (entries 4 and 5) were higher than those in CH_2Cl_2 (entries 1−3). These results suggest that the degree of polymerizations (DP_n) may be influenced by the solvent, resulting in a higher DP_n in toluene. We selected polymer **4** obtained from entry 5 (Table 1) to be analyzed and converted to DHPC in the subsequent experiments from the viewpoint of DP_n. ^{13}C NMR spectrum of polymer **4** (entry 5) having $[\alpha]_D$ −4.3° shows that the polymer obtained has a high degree of stereoregularity, that is, exactly

Table 1. Polymerization of 3-*O*-Benzyl-6-*O*-dihydrophytyl-α-D-glucopyranose 1,2,4-Orthopivalate (**3**)[a]

entry	temp °C	$[M]_0$[b] M	solvent	yield[c] %	$10^{-3}M_n$[d]	M_w/M_n[d]	DP_n
1	−30	1.0	CH_2Cl_2	90	3.4	1.8	5.5
2	0	1.0	CH_2Cl_2	78	9.6	1.9	15.6
3	20	1.0	CH_2Cl_2	91	3.7	1.4	6.0
4	0	1.0	toluene	76	14.0	1.8	23.0
5	0	2.0	toluene	85	22.0	1.8	35.9

[a] Catalyst: BF_3-Et_2O (5 mol %); polymerization time = 48 h. [b] Initial monomer concentration. [c] The polymer was the insoluble fraction in chloroform/*n*-hexane (1/15, v/v). [d] Estimated from GPC eluted with $CHCl_3$ based on polystyrene standards.

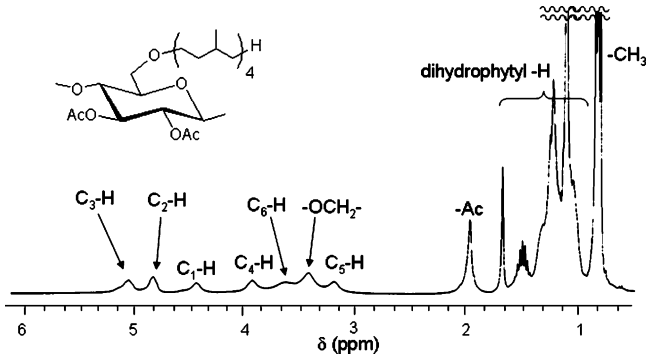

Figure 2. ^{1}H NMR spectrum of polymer **5**.

cellulose derivatives. The anomeric peak of the stereoregular polymer **4** appears at 100.1 ppm as a sharp singlet. We converted the polymer **4** to polymer **5** via depivaloylation, debenzylation, and acetylation. ^{1}H NMR spectrum of polymer **5** is shown in Figure 2. The ^{1}H resonances for all ring protons were assigned, indicating high stereoregularity. Then, the polymer **5** was converted to DHPC. ^{13}C NMR spectrum of DHPC also indicates high stereoregularity, whereas ^{1}H NMR spectrum is not clear, since the resonances for ring protons are close each other. We used this DHPC for the preparation of the LB films.

6-*O*-Alkylcelluloses CC and SC were prepared by the same procedures as reported.[40] The molecular weight and DP_n of CC were 2.9×10^4 and 51.7, and those of SC were 2.7×10^4 and 45.3.

***π*−*A* Isotherms for 6-*O*-Alkylcelluloses.** The cellulose derivatives SC, CC, and DHPC were spread onto a water surface from chloroform/methanol (20:1) mixed solutions, and the *π*−*A* isotherms were measured at 20 °C (Figure 3). The surface pressure begins to increase at an area of ca. 0.9 nm^2 per anhydrous glucose unit (AGU) for DHPC, whereas it increases at an area of ca. 0.8 nm^2 per AGU for CC and SC. The *π*−*A* isotherm for CC shows a typical well-developed plateau region, indicating the transition from a monolayer to a bilayer structure as reported by Itho et al.[13] Thus, CC is not suitable for preparing the monolayer film. The *π*−*A* isotherms for both DHPC and SC give a steep increase and exhibit high collapse pressure without phase transition, meaning that highly condensed monolayers are formed. These indicate that the hydrophobicity of the substituents considerably contributes to form stable condensed-type films. The limiting surface areas per AGU estimated by extrapolating the steepest tangent of the isotherm to zero surface pressure are 0.55 nm^2 per AGU for SC[30] and 0.72 nm^2 for DHPC. Since the limiting area of cellulose tristearate was reported to be under 0.7 nm^2 per AGU at 20 °C,[13] the observed area of DHPC is obviously due to the branched methyl group of dihydrophytyl group.

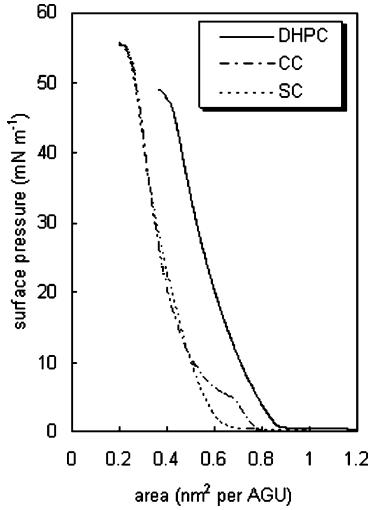

Figure 3. *π*−*A* isotherms of 6-*O*-alkylcellulose monolayers at 20 °C.

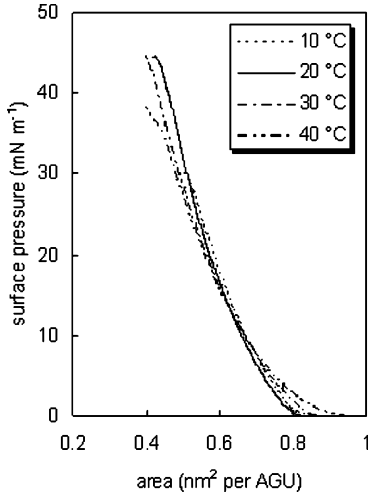

Figure 4. Temperature dependence of *π*−*A* isotherms for DHPC.

To investigate the stability of a monolayer, we studied the temperature dependence of the *π*−*A* isotherms for DHPC (Figure 4). The *π*−*A* isotherms for SC show plateau regions at 30−40 °C as already reported, indicating the main phase transition from a fluidlike to a condensed monolayer.[30] On the other hand, the *π*−*A* isotherms for DHCP show a solid condensed monolayer without phase transition even at 30−40 °C, indicating that the phase transition of DHPC is not dependent on the subphase temperature from 10 to 40 °C. Poor dependence of a DHPC monolayer on temperature suggests that the cohesive force of DHPC is higher than that of SC, irrespective of the steric hindrance caused by the extra methyl groups.

Moreover, we investigated the shape of the isotherms depending on the time that a monolayer remained in its uncompressed state. Goldenberg et al. reported that an isotherm shifts to a higher area when the floating layer is allowed to remain uncompressed for a long time and is generally stabilized after ca. 1.5−2 h in the uncompressed state.[41] Figure 5 shows the *π*−*A* isotherms for both DHPC and SC prepared by compression after a constant time. The limiting surface areas of SC are ca. 0.55 and ca. 0.6 nm^2 per AGU in the uncompressed states of 30 and 120 min, respectively. This difference of the surface areas between the two indicates that a true floating SC monolayer, which is an equilibrium state of a monolayer for the occupied molecular area, is only obtained when sufficient time is allowed before compression. On the other hand, the limiting surface areas of DHPC are ca. 0.72 and 0.73 nm^2 per

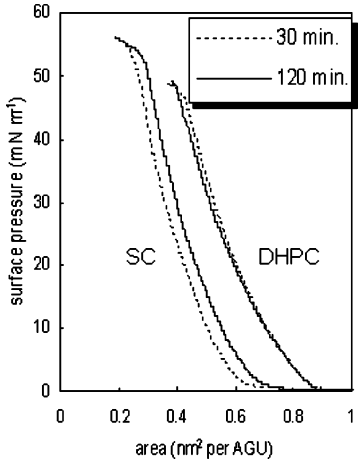

Figure 5. $\pi-A$ isotherms for DHPC and SC; the times before compression are indicated.

AGU in the uncompressed states of 30 and 120 min, respectively. This indicates that a true floating DHPC monolayer is formed in the uncompressed state of 30 min. We suggest that dihydrophytyl group helps in the formation of a true floating monolayer.

AFM Images of Monolayer Films. Atomic force microscopy (AFM) provides direct information on the morphology of a surface monolayer.[42] Figure 6a−c shows AFM images of monolayer films transferred at 0, 10, and 30 mN m^{-1} at 20 °C after the uncompressed state of 30 min, respectively. A DHPC monolayer was transferred by the upward stroke with a transfer ratio of almost unity onto mica, but was not transferred by the downward stroke. At 0 mN m^{-1}, where the isotherm is just about to rise, the fractions of holes are observed, and a heterogeneous film consisting of aggregates with nonuniform size can be seen. The film thickness at 0 mN m^{-1} is estimated to be about 2.6 nm by the height of the substance in comparison with the bottom. The value is in good agreement with that of the molecular model for DHPC. This suggests that a glucopyranose ring lies flat on the water surface, and the alkyl side chains, fully extended, stand normal to the ring, as reported by Itoh et al.[13] At 10 mN m^{-1}, the fractions of holes decrease considerably, and the presumed film thickness is estimated to be about 2.4 nm. At 30 mN m^{-1}, a perfect homogeneous monolayer is obtained. The film thickness, however, cannot be estimated, since the gap between the substance and the bottom is indistinct. With further compression, a homogeneous monolayer is gradually collapsed. On the basis of these images obtained, the most suitable surface pressure is 30 mN m^{-1} to transfer a homogeneous monolayer onto a substrate.

The root-mean-square (rms) surface roughness of the monolayer transferred at 30 mN m^{-1} is 1.22 Å. This value is approximately equal to the rms surface roughness of mica (1.36 Å) and obviously smaller than the rms roughness at 10 mN m^{-1} (5.40 Å), indicating that a homogeneous monolayer is formed at 30 mN m^{-1}. On the basis of these observations, the optimum surface pressure to prepare homogeneous LB films of DHPC is determined to be 30 mN m^{-1}.

As already reported,[30] SC on a water surface forms a homogeneous monolayer at 10 mN m^{-1}. Thus, the following picture about DHPC can be envisaged: The molecules which originally stand up on the surface at 0 mN m^{-1} come closer to each other by compressing, and then, a homogeneous monolayer is formed at 30 mN m^{-1}. The occupied area of DHPC is 0.57 nm^2 per AGU at 30 mN m^{-1}, whereas that of SC is 0.55 nm^2 per AGU at 10 mN m^{-1}. Both values favorably agree with the cross section of a glucopyranose ring. Herein, a homogeneous monolayer would be formed when the occupied area per AGU is identical with the value at the cross section of a glucopyranose ring.

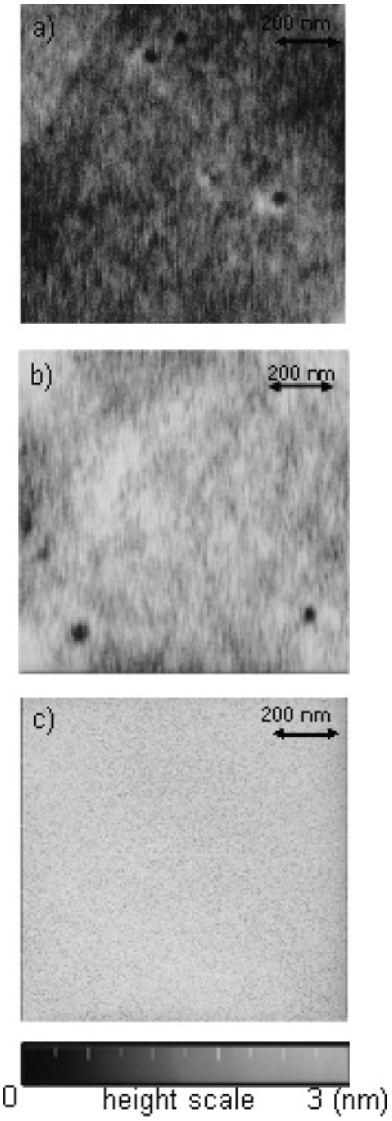

Figure 6. AFM images of DHPC monolayer transferred at the surface pressures of (a) 0 mN m^{-1}; (b) 10 mN m^1; (c) 30 mN m^{-1}; all at 20 °C.

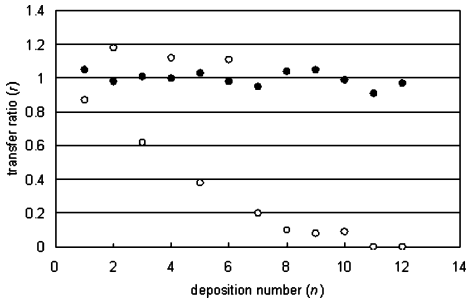

Figure 7. Transfer ratio as a function of deposition number for DHPC at two different surface pressures. Solid circle (●), at 30 mN m^{-1}; open circle (○), at 10 mN m^{-1}.

Fabrication of LB Films of DHPC. We then tried to transfer a DHPC monolayer to a hydrophobic CaF_2 substrate. Figure 7 shows typical transfer ratios for DHPC. A SC monolayer was transferred only by the upward stroke at a pressure of 10 mN m^{-1} by applying the improved method, but not by the down

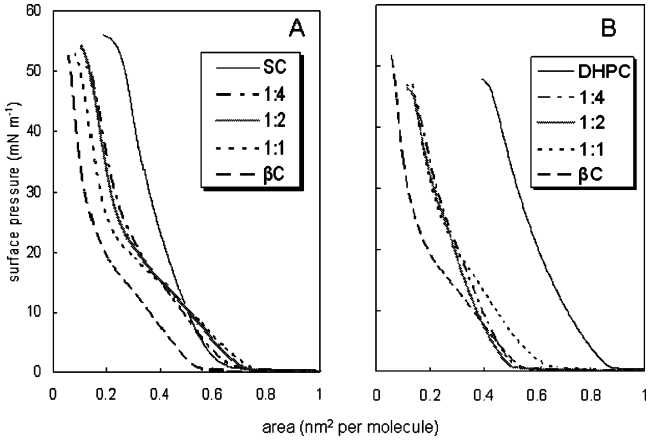

Figure 8. $\pi-A$ isotherms of βC−SC mixed monolayers (A) and βC−DHPC mixed monolayers (B) with molar ratio indicated.

stroke, that is, Z-type deposition.[30] On the basis of these results, we preliminarily tried to prepare the LB films of DHPC at a pressure of 10 mN m^{-1}. The monolayer transfer was, however, unsuccessful, regardless of several attempts to improve transfer ratios by varying the temperature (10−30 °C) or the dipping speed. Then, we considered the stabilization pressure and found that the monolayer transfer was successful only at a pressure of 30 mN m^{-1}. Furthermore, LB films of DHPC could be prepared with the transfer ratios of almost unity without carrying out the complicated technique.[30] Zhang et al. also reported that the transfer behavior of cellulose derivatives depends on the surface pressure.[43] Consequently, we successfully prepared LB films of DHPC onto a CaF_2 substrate.

In the same way, a DHPC monolayer was successfully transferred onto mica, quartz, and a gold-evaporated slide glass, whereas not onto a silicon wafer. This is presumably because a silicon wafer has a smoother surface than quartz, though it would be similar to mica and quartz in terms of hydrophobicity and (almost) chemistry.

Mixed Monolayers of β-Carotene and DHPC. Figure 8 shows the $\pi-A$ isotherms of the monolayers of βC mixed with SC (panel A) and with DHPC (panel B) in several molar proportions. The limiting molecular area of pure βC is 0.18 nm^2 per molecule by the extrapolation of the steepest part of the isotherm. This value is similar to that of Leblanc and Orger:[44] The βC molecules stand perpendicular to the water surface. The $\pi-A$ isotherm for βC suggests that compression of the monolayer to the surface pressures until 20 mN m^{-1} results in the gradual orientation of molecules at the interface, and then, the βC molecules are oriented vertically at the interface above it. We tried to prepare the LB films of βC, but the monolayer on a water subphase collapsed when compression stopped, since it is unstable due to the absence of a hydrophilic group.[44] On the other hand, the mixed monolayers of βC−cellulose derivatives (SC and DHPC) did not collapse rapidly. This is presumably because βC molecules are supported by the long alkyl chain of cellulose derivatives.

The behaviors of the $\pi-A$ isotherms for βC−cellulose derivatives are different (Figure 8). The isotherms for βC−DHPC follow near the pure βC isotherm, whereas those for βC−SC are near the intermediate line between the pure βC and SC isotherms. In general, the experimentally obtained $\pi-A$ isotherms for the pure component make it possible to predict the mean molecular area in the mixed monolayer.[45] When the two components are immiscible or form an ideal two-dimensional solution, the mean molecular area plot is theoretically calculated. On the other hand, the mean molecular area is positively or negatively deviated away from the theoretical isotherm; one or both components occupies a larger or smaller area per molecule than its pure components. In other words, the mutual interaction affects the positive or negative deviations of the $\pi-A$ isotherms. The isotherms for βC−HPC are negatively deviated in the entire range of surface pressure, indicating that βC and DHPC molecules are stacking on each other and condensation or aggregation can take place. On the contrary, the isotherms for βC−SC are positively deviated below about 20 mN m^{-1} and show slightly positive deviation above 20 mN m^{-1}, indicating that a repulsive-type interaction between βC and SC occurs especially at a lower pressure. These results indicate that the branched dihydrophytyl group of DHPC can interact with βC more effectively than the normal stearyl group of SC.

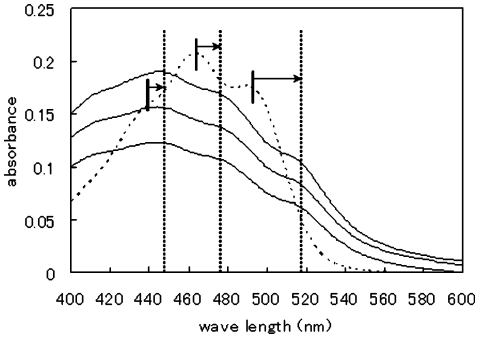

Figure 9. UV−vis absorption spectra of βC−DHPC (1:2) LB films as a function of deposited layers. Solid curves: 11, 13, and 15 layers LB films from bottom up. Dashed curve: the chloroform solution of βC−DHPC (1:2).

When the mixture ratios of βC−DHPC are 1:2 and 1:4, no expanded behavior is observed below 20 mN m^{-1}, and the isotherms show steep increases in surface pressure. On the basis of these results, the optimum mixture ratios of βC−DHPC are 1:2 or 1:4 to prepare a stacking monolayer.

A monolayer of βC−DHPC was transferred at 30 mN m^{-1} onto a freshly cleaved mica by the upward stroke during the vertical dipping method. Transfer ratios were almost unity. The AFM image was relatively smooth and homogeneous. The rms surface roughness of the monolayer was 1.65 Å, indicating that the monolayer is smooth and homogeneous.

Fabrication of LB films of βC−DHPC. A monolayer of βC−DHPC (1:2 and 1:4) was successively transferred at 30 mN m^{-1} on several substrates at 20 °C as a Y-type film without exfoliation. If the substrate was hydrophilic, e.g., quartz, the first monolayer was transferred only by the upward stroke, whereas the successive monolayers were constantly transferred onto the substrate at both lifting/dipping processes. The transfer ratios yielded ca. 1.1 for the first monolayer transferred by the upward stroke and almost unity for the successive monolayer. On the other hand, if the substrate was hydrophobic, the monolayer was transferred from the first downward stroke, and the transfer ratios yielded almost unity.

Characterization of LB Films. Figure 9 shows the UV−vis absorption spectra of the LB films of βC−DHPC. It has been known that a chloroform solution of βC exhibits three absorption peaks in the vicinity of 450 nm.[29] The absorption peaks of LB films are observed at 447, 476, and 514 nm, and these values are almost similar to those of Matsuura et al.[29] The absorption intensity of these peaks increases almost proportionally with the number of layers of the LB films. This observation indicates that the structure of the LB films changes little with the number of layers. The peaks of the LB films shift

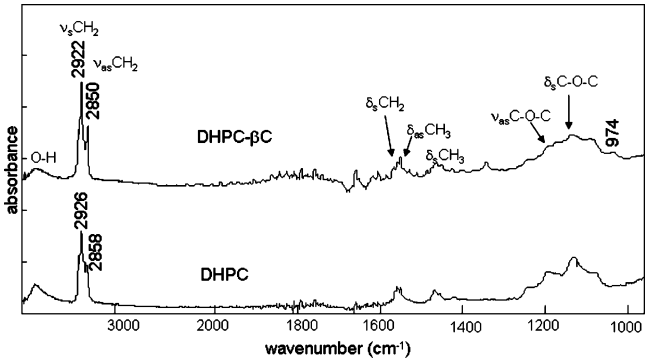

Figure 10. Infrared transmission spectra of 12-layer LB films of DHPC (lower) and 18-layer LB films of βC−DHPC (upper) deposited on CaF_2.

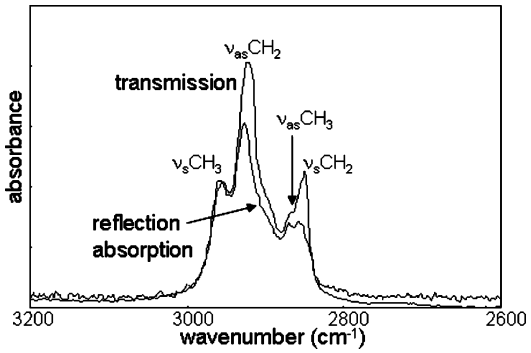

Figure 11. The expanded infrared spectra of βC−DHPC at around 2600−3200 cm^{-1}.

to the longer wavelength (ca. 10−15 nm), i.e., a red shift, as compared with those in chloroform solution. This is because a strong intermolecular interaction caused by a shortening of the molecular spacing induces a decrease of the energy gap.[29] The LB films of βC−DHPC, therefore, would be a high-density packing film in the in-plane directions as reported by Matsuura et al.[29]

Fourier transform infrared (FT-IR) spectra, which afford structural information such as molecular orientation, were measured for the LB films of βC−DHPC (1:4). Figure 10 shows the IR transmission spectra of the LB films of pure DHPC (20 layers) and βC−DHPC (1:4, 18 layers). Bands at 2926 and 2858 cm^{-1} of DHPC and at 2922 and 2850 cm^{-1} of βC−DHPC are assigned to CH_2 antisymmetric and symmetric stretching modes of the hydrocarbon chains, respectively. It is well-known that the hydrocarbon chains are highly ordered (in all trans-zigzag conformation) when the frequencies of the CH_2 antisymmetric (∼2920 cm^{-1}) and symmetric (∼2850 cm^{-1}) stretching modes are lower than before.[46] The bands of βC−DHPC appear at the lower frequencies than the pure DHPC, suggesting that βC molecules are interdigitated with DHPC molecules and the monolayers of βC−DHPC are highly ordered in all trans-zigzag conformation. The infrared spectrum of βC is expected to show the peaks assigned to weak C−H stretching (3028 cm^{-1}), weak C═C stretching (1550−1650 cm^{-1}), and strong C−H bending (966 cm^{-1} for trans-double bond). In this spectrum, however, an only C−H bending peak is detected at 974 cm^{-1} because of its small existence.

Figure 11 shows the expanded transmission spectrum and RAS of the LB films of βC−DHPC (1:4) at around 2600−3200 cm^{-1}. It is well-known that vibrational modes with their transition moments perpendicular to the surface are enhanced in a RAS.[47,48] Hereby, the molecular orientation of hydrocarbon chains can be investigated by comparing the intensities of CH_2

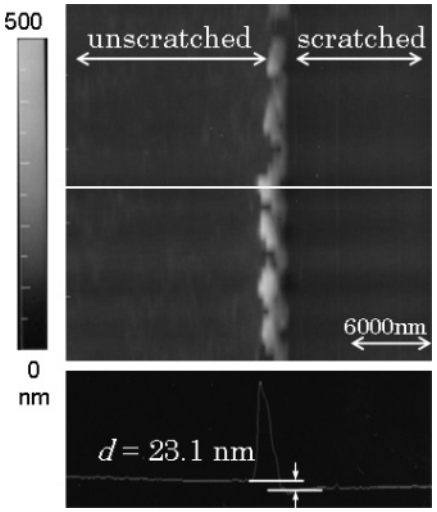

Figure 12. AFM image of the scratched βC−DHPC (1:4) LB films and height profile on the line indicated scan on the surface.

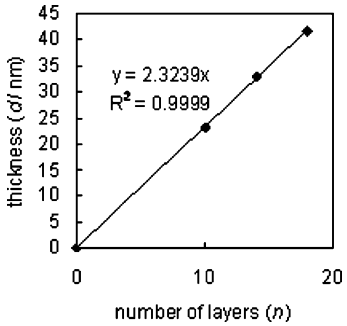

Figure 13. Film thickness plotted against the number of deposition determined by AFM.

antisymmetric and symmetric stretching bands between the transmission spectra and RAS. In Figure 11, the intensities of the two CH_2 stretching bands are much stronger in the transmission spectrum than in the RAS. This indicates that the dihydrophytyl chains are nearly directed perpendicular to the substrate.

We measured the thickness of the LB films of βC−DHPC on a silicon substrate by AFM measurements according to the previous procedure.[30] The thicknesses of 10, 14, and 18 layers were determined by AFM imaging across the scratch boundary as shown in Figure 12. Figure 13 shows plots of the thickness (d) as a function of number of layers (n). The LB films are of high quality, because the thickness increases well in proportion to the number of layers. The thickness per layer is calculated to be 2.32 nm from the slope of the line. This suggests that the dihydrophytyl chain would stand almost perpendicular to the glucose ring, since the maximum length of the dihydrophytyl chain with a trans-zigzag conformation is estimated to be ca. 2.0 nm (C−C distance = 0.154 nm, C−C−C angle = 109.28°). On the other hand, the molecular length of βC is estimated to be ca. 3.0 nm.[29] Thus, the βC molecules in the LB films are to some extent tilted to the plane, suggesting that they fill in the empty space of the dihydrophytyl chains.

Conclusions

Here, we proposed a novel approach to construct cellulose LB films containing β-carotene. The cellulose derivative with dihydrophytyl group at the 6-O position, 6-*O*-dihydrophytylcellulose (DHPC), was synthesized via a ring-opening polym-

erization. DHPC formed a homogeneous monolayer at 30 mN m^{-1} either alone or with β-carotene. DHPC has three characteristics in $\pi-A$ measurement compared with CC and SC: (1) The isotherm for DHPC gave a steep increase and high collapse pressure in contrast to that of CC; (2) the limiting area of DHPC was 0.72 nm^2 per AGU and similar to that of cellulose tristearate (0.7 nm^2 per AGU),[13] though that of SC was 0.55 nm^2 per AGU; (3) the behavior of a DHPC monolayer at an air−water interface was independent of the temperature of the water subphase, and the time that a true floating monolayer is formed in its uncompressed state was around 30 min, though those of SC were dependent. DHPC could be transferred successfully at 30 mN m^{-1} and 20 °C onto solid substrates such as mica, quartz, CaF_2, and a gold-evaporated slide glass except a silicon wafer.

The preparation and characterization of βC−DHPC monolayer and multilayer films were studied in detail. The $\pi-A$ isotherms for βC−DHPC were negatively deviated in the entire range of surface pressure, indicating that βC and DHPC molecules were stacking on each other. On the other hand, those for βC−SC were positively deviated, indicating that SC could not anchor βC well. Therefore, DHPC has the ability to anchor βC on the basis of these results, because they both have isoprenoid moieties as a common structure. The transfer ratios in the preparation of the LB films of βC−DHPC were almost unity. The absorbance of UV spectra increased linearly as the number of layers increased. The CH_2 antisymmetric and symmetric stretching modes indicated that the hydrocarbon chains in the LB films of βC−DHPC had an approximately all-trans zigzag conformation. The dihydrophytyl chains were fairly directed perpendicular to the substrate by comparison between transmission spectrum and RAS. AFM section analysis revealed the thickness per layer to be 2.32 nm, indicating that the dihydrophytyl chains stood almost perpendicular and the βC molecules were rather tilted.

Consequently, DHPC was found to be an appropriate matrix to fabricate the mixed LB films containing βC. Chlorophyll a may be anchored using DHPC in the films since it has an isoprenoid moiety, too. In the future, β-carotene molecules would make it possible to pass a photocurrent through the cellulose LB films.

Acknowledgment. This investigation was supported in part by a Grant-in-Aid for Scientific Research from the Ministry of Education, Science, and Culture of Japan (no. 17380107).

References and Notes

(1) Harkness, B. R.; Gray, D. G. *Macromolecules* **1990**, *23*, 1452−1457.
(2) Schaub, M.; Wenz, G.; Wegner, G.; Stein, A.; Klemm, D. *Adv. Mater.* **1993**, *5*, 919−922.
(3) Hoenich, N. A.; Stamp, S. *Biomaterials* **2000**, *21*, 317−324.
(4) Tiller, J.; Berlin, P.; Klemm, D. *Macromol. Chem. Phys.* **1999**, *200*, 1−9.
(5) Kubota, T.; Kusano, T.; Yamamoto, C.; Okamoto, Y. *Chem. Lett.* **2001**, *7*, 724−725.
(6) Holzer, W.; Penzkofer, A.; Redl, F. X.; Lutz, M.; Daub, J. *Chem. Phys.* **2002**, *282*, 88−99.
(7) Hanemann, O.; Ballauff, M. *Macromolecules* **1997**, *30*, 7638−7640.
(8) Klemm, D.; Heinze, T.; Philipp, B.; Wagenknecht, W. *Acta Polym.* **1997**, *48*, 277−297.
(9) Redl, F. X.; Köthe, O.; Röckl, K.; Bauer, W.; Daub, J. *Macromol. Chem. Phys.* **2000**, *201*, 2091−2100.
(10) Redl, F. X.; Lutz, M.; Daub, J. *Chem.−Eur. J.* **2001**, *24*, 5350−5358.
(11) Kawaguchi, T.; Nakahara, H.; Fukuda, K. *Thin Solid Films* **1985**, *133*, 29−38.
(12) Miyashita, T. *Prog. Polym. Sci.* **1993**, *18*, 263−294.
(13) Itoh, T.; Tsujii, Y.; Suzuki, H.; Fukuda, T.; Miyamoto, T. *Polym. J.* **1992**, *24*, 641−652.
(14) Ifuku, S.; Tsujii, Y.; Kamitakahara, H.; Takano, T.; Nakatsubo, F. *J. Polym. Sci., Part A: Polym. Chem.* **2005**, *43*, 5023−5031.
(15) Schaub, M.; Fakirov, C.; Schmidt, A.; Lieser, G.; Wenz, G.; Wegner, G.; Albouy, P.-A.; Wu, H.; Foster, M. D.; Majrkzak, C.; Satija, S. *Macromolecules* **1995**, *28*, 1221−1228.
(16) Leblanc, R. M.; Konka, V. *Surfactant Sci. Ser.* **2001**, *95*, 641−648.
(17) Guay, D.; Leblanc, R. M. *Langmuir* **1987**, *3*, 575−580.
(18) Picard, G.; Munger, G.; Leblanc, R. M.; Lesage, R.; Sharma, D.; Siemiarczuk, A.; Bolton, J. R. *Chem. Phys. Lett.* **1986**, *129*, 41−47.
(19) Sato, H.; Ozaki, Y.; Oishi, Y.; Kuramori, M.; Suehiro, K.; Nakashima, K.; Uehara, K.; Iriyama, K. *Langmuir* **1997**, *13*, 4676−4682.
(20) Sato, H.; Oishi, Y.; Kuramori, M.; Suehiro, K.; Kobayashi, M.; Uehara, K.; Araki, T.; Iriyama, K.; Ozaki, Y. *J. Chem. Soc., Faraday Trans.* **1997**, *93*, 621−627.
(21) Nam, Y. S.; Kim, J. M.; Choi, J.-W.; Lee, W. H. *Mater. Sci. Eng., C* **2004**, *24*, 35−38.
(22) Barazzouk, S.; Kamat, P. V.; Hotchandani, S. *J. Phys. Chem. B* **2005**, *109*, 716−723.
(23) Agostiano, A.; Catucci, L.; Colagemmina, G.; Scheer, H. *J. Phys. Chem. B* **2002**, *106*, 1446−1454.
(24) Buoninsegni, F. T.; Becucci, L.; Moncelli, M. R.; Guidelli, R.; Agostiano, A.; Cosma, P. *J. Electroanal. Chem.* **2003**, *550−551*, 229−240.
(25) Agostiano, A.; Catucci, L.; Colafemmina, G.; Monica, M. D.; Scheer, H. *Biophys. Chem.* **2000**, *84*, 189−194.
(26) Pan, J.; Xu, Y.; Sun, L.; Sundström, V.; Polívka, T. *J. Am. Chem. Soc.* **2004**, *126*, 3066−3067.
(27) Miyasaka, T.; Watanabe, T.; Fujishima, A.; Honda, K. *J. Am. Chem. Soc.* **1978**, *100*, 6657−6665.
(28) Miyasaka, T.; Watanabe, T.; Fujishima, A.; Honda, K. *Nature (London)* **1979**, *277*, 638−640.
(29) Matsuura, T.; Nishimura, A.; Shimoyama, Y. *Jpn. J. Appl. Phys.* **2000**, *39*, 3557−3561.
(30) Ifuku, S.; Nakai, S.; Kamitakahara, H.; Takano, T.; Tsujii, Y.; Nakatsubo, F. *Biomacromolecules* **2005**, *6*, 2067−2073.
(31) Ion, A.; Partali, V.; Sliwka, H.-R.; Banica, F. G. *Electrochem. Comm.* **2002**, *4*, 674−678.
(32) Miyahara, T.; Kurihara, K. *J. Am. Chem. Soc.* **2004**, *126*, 5684−5685.
(33) Davisson, V. J.; Woodside, A. B.; Neal, T. R.; Stremler, K. E.; Muehlbacher, M.; Poulter, C. D. *J. Org. Chem.* **1986**, *51*, 4768−4779.
(34) Ishiwatari, M.; Yamada, K.; Ishiwatari, R. *Chem. Lett.* **2000**, *2000*, 206−207.
(35) Ejaz, M.; Ohno, K.; Tsujii, Y.; Fukuda, T. *Macromolecules* **2000**, *33*, 2870−2874.
(36) Tsujii, Y.; Itoh, T.; Fukuda, T.; Miyamoto, T.; Ito, S.; Yamamoto, M. *Langmuir* **1992**, *8*, 936−941.
(37) Karakawa, M.; Nakatsubo, F. *Carbohydr. Res.* **2002**, *337*, 951−954.
(38) Nakatsubo, F.; Kamitakahara, H.; Hori, M. *J. Am. Chem. Soc.* **1996**, *118*, 1677−1681.
(39) Karakawa, M.; Kamitakahara, H.; Takano, T.; Nakatsubo, F. *Biomacromolecules* **2002**, *3*, 538−546.
(40) Nakai, S.; Kamitakahara, H.; Takano, T.; Nakatsubo, F.; Siegmund, G.; Klemm, D. *Proceedings of the 1st International Cellulose Conference*; Kyoto, Japan, 2002; p 124.
(41) Goldenberg, L. M.; Cooke, G.; Petty, M. C. *Mater. Sci. Eng., C* **1998**, *5*, 281−284.
(42) Itoh, T.; Tsujii, Y.; Fukuda, T.; Miyamoto, T. *Langmuir* **1991**, *7*, 2803−2807.
(43) Zhang, Y.; Tun, Z.; Ritcey, A. M. *Langmuir* **2004**, *20*, 6187−6194.
(44) Leblanc, R. M.; Orger, B. H. *Biochim. Biophys. Acta* **1972**, *275*, 102−104.
(45) Cadenhead, D. A.; Müller-Landau, F. *J. Colloid Interface Sci.* **1980**, *78*, 269−270.
(46) Katayama, N.; Ozaki, Y.; Araki, T.; Iriyama, K. *J. Mol. Struct.* **1991**, *242*, 27−37.
(47) Miyashita, T.; Suwa, T. *Langmuir* **1994**, *10*, 3387−3389.
(48) Zhao, B.; Li, H.; Zhang, X.; Shen, J.; Ozaki, Y. *J. Phys. Chem. B* **1998**, *102*, 6515−6520.

BM060083X